



OPEN Pentraxin3 exacerbates acute pancreatitis injury by inhibiting oxidative phosphorylation pathway

Wenyue Wang^{1,2,4}, Yaning Wang^{1,4}, Chenchen Yuan^{1,2}, Fei Cao^{1,2}, Weisong Tang^{1,2}, Qingtian Zhu¹, Xiaowu Dong^{1,2}, Lihui Deng³, Guotao Lu¹, Qing Xia³ & Weiwei Chen^{1,2}✉

Local pancreatic necrosis and systemic inflammatory response caused by acute pancreatitis (AP) are closely related to the disease prognosis and severity. This study aimed to explore whether pentraxin 3 (PTX3) regulates AP pancreatic necrosis and reveals the underlying mechanism. By using AP time gradient transcriptomics, proteomics and liquid phase chip analysis, we found a close association between PTX3 and AP. Subsequently, caerulein (CAE) induced in vivo AP model and CCK induced in vitro acinar cell damage model were constructed to determine the expression of PTX3 and its regulation of AP. The results showed that PTX3 was highly expressed in the CAE-induced AP model. And more severe pancreatic tissue damage and increased serum amylase were observed after the intervention of recombinant protein PTX3, which was strongly linked to the decreasing in mitochondrial membrane potential, increasing in reactive oxygen species, and regulation by oxidative phosphorylation pathway. PTX3 could exacerbate acinar cell damage in AP by mediating the process of oxidative phosphorylation.

Keywords Acute pancreatitis, Pentraxin 3, Acinar cell injury, Oxidative phosphorylation, Reactive oxygen species

Acute pancreatitis (AP) is a serious gastrointestinal disorder characterized by acinar cell injury caused by the pathological activation of trypsinogen¹. Approximately 20% of individuals with AP experience extensive pancreatic or peripancreatic necrosis, leading to a mortality rate ranging from 30 to 39% in cases of infectious necrosis². Pancreatic necrosis profoundly impacts the prognosis and quality of life of patients with AP, creating substantial economic and social burdens. Presently, clinical drug trials for AP are restricted, and effective preventive and treatment strategies for pancreatic necrosis remain elusive³. Thus, investigating the primary mediators and molecular pathways of AP is essential for addressing clinical challenges.

In a prior investigation, we obtained plasma samples from 70 acute pancreatitis patients and identified pentraxin 3 (PTX3) as a promising marker for early detection of severe acute pancreatitis⁴. Prior studies have demonstrated that Pentraxins are an evolutionarily conserved superfamily of pattern recognition molecules (PRMs) in the innate immune system. This superfamily is divided into two subclasses: the classical short-chain protein C-reactive protein and the long-chain protein PTX3, which plays a crucial role in modulating innate immunity and inflammation⁵. For instance, in a model of ischemic acute kidney injury, the homozygous knockout of PTX3 in mice ameliorated renal damage⁶, whereas overexpression of PTX3 exacerbated the severity of ventilator-induced lung injury⁷. Studies have shown that PTX3 plays an important role in endoplasmic reticulum stress induced by tunicamycin. This indicates that in retinal pigment epithelial cells, endoplasmic reticulum stress can up-regulate the expression of PTX3⁸.

However, previous studies have not investigated the role of PTX3 in acinar cell damage and its associated molecular mechanisms. Through a comprehensive multi-omics analysis in this study, we identified PTX3 as a potential key player in acinar cell necrosis. Our research applied proteomic and molecular biology techniques to thoroughly explore how PTX3 exacerbates acinar cell necrosis in AP.

¹Pancreatic Center, Department of Gastroenterology, Yangzhou Key Laboratory of Pancreatic Disease, Institute of Digestive Diseases, The Affiliated Hospital of Yangzhou University, Yangzhou, Jiangsu, China. ²Medical College of Yangzhou University, Yangzhou, Jiangsu, China. ³West China Centre of Excellence for Pancreatitis, Institute of Integrated Traditional Chinese and Western Medicine, Sichuan Provincial Pancreatitis Centre and West China-Liverpool Biomedical Research Centre, West China Hospital, Sichuan University, Chengdu, Sichuan, China. ⁴Wenyue Wang and Yaning Wang contributed equally. ✉email: cww1984@126.com

Materials and methods

Animals and ethics

The C57BL/6J strain mice (25–30 g) were procured from the Model Animal Research Center of Nanjing University (Nanjing, China). The mice were housed in specific pathogen-free (SPF) facilities and fed a standard rodent diet. The lighting regime was set at a 12-hour light-dark cycle, while the temperature in the housing area was maintained at $25^{\circ}\text{C} \pm 2^{\circ}\text{C}$. This study received approval from the Science and Technology Commission of the Medical College of Yangzhou University (YXYLL-2024-074) and strictly adhered to the guidelines for experimental animal care (NIH Publication No.85–3, revised in 1996).

Acute pancreatitis model induced by caerulein (CAE)

The C57BL/6J mice were randomly allocated into three groups: control, model, and rPTX3 groups (5, 10, 20 $\mu\text{g}/\text{kg}$). In the model group, mice received intraperitoneal injections of CAE (150 $\mu\text{g}/\text{kg}$, 1-hour interval, 10 times). One hour after CAE injection, the rPTX3 group received the injection of PTX3 recombinant protein, while the control group was administered an equivalent volume of PBS.

Pancreatic histopathology evaluation

Following fixation, dehydration, and embedding in wax, pancreatic tissues were stained with hematoxylin and eosin. Subsequently, we evaluated the histomorphology features, such as necrosis of acinar cells, infiltration of inflammatory cells, and edema in the tissue⁹.

Determination of serum enzymology by ELISA

The Mouse Pentraxin 3/TSG-14 Quantikine ELISA Kit (Catalog No. MPTX30, R&D Systems) was employed to determine the serum concentration of PTX3 in mice. Meanwhile, serum amylase (Biotechnology&Science Inc.), lipase (Nanjing Jiancheng Corp.) levels were measured.

Isolation and processing of pancreatic acinar cells

Collagenase I (Sigma-Aldrich) was injected into the pancreatic tissue through the main pancreatic duct to digest and extract mouse pancreatic acinar cells. Subsequently, the isolated cells were incubated at 37°C in HEPES (Sigma-Aldrich) buffer. Utilizing CCK stimulation for 6 h, we established an in vitro model for acinar damage¹⁰. Finally, both the cells and the supernatants were harvested for subsequent analysis.

LDH release assay

Mouse pancreatic acinar cells were evaluated following the experimental protocols outlined by the manufacturer of the LDH release kit (LDH Cytotoxicity Assay Kits, Beyotime Biotechnology).

Calcein-AM/PI double staining method

Pancreatic acinar cells were double-stained with Calcein-AM (2mM, strong green fluorescence for live cells) and PI (1.5mM, red fluorescence for dead cells). The staining working solution was prepared by mixing Calcein-AM solution, PI solution, and 5 mL of $1\times$ Assay Buffer. The collected acinar cells were centrifuged to remove the supernatant, washed with $1\times$ Assay Buffer, and resuspended in 200 μL of $1\times$ Assay Buffer. The staining working solution was added, and the cells were incubated at 37°C for 15 min. After incubation, the cells were observed and photographed using a laser confocal microscope.

Mitochondrial membrane potential assessment

The mitochondrial membrane potential determination was conducted following the protocol specified by the manufacturer of the Mitochondrial Membrane Potential Kit (JC-1 Mitochondrial Membrane Potential Assay Kit, HY-K0601, MCE).

Multi-omics combined analysis

RNA sequencing, quality control, and analysis

Pancreatic tissue samples collected at 0 h, 3 h, 6 h, and 12 h induced by CAE were subjected to RNA-Seq analysis. RNA integrity and quantity were precisely determined using the Agilent 2100 bioanalyzer, initiating the RNA analysis from total RNA. Illumina sequencing was employed for generating 150 bp paired-end reads after the library was prepared.

Quality control procedures included converting sequenced image data into fastq format, filtering out reads with adaptors, those containing uncertain bases (N), and low-quality reads (bases with $Q_{\text{phred}} \leq 20$ contributing to over 50% of the read length). The clean data's quality was evaluated by calculating parameters such as Q20, Q30, and GC content. Subsequently, the reference genome index was constructed using HISAT2 v2.0.5 to align the paired-end clean reads.

Each gene's read count was determined using feature Counts, followed by the calculation of FPKM values. Differential expression analysis between various comparison combinations was carried out using the DESeq2 program package in RStudio ($p\text{-value} < 0.05$, $|\log_2\text{FC}| \geq 1$), utilizing a negative binomial distribution model for identifying differentially expressed genes. To control false positive rates, P-values were adjusted using the Benjamini.

KEGG and GO pathway enrichment analysis

We conducted pathway enrichment analysis of the Gene Ontology (GO) and Kyoto Encyclopedia of Genes and Genomes (KEGG) signaling pathways utilizing the DAVID database.

Short time-series expression miner (STEM) analysis

The STEM program was utilized to examine trends in gene expression over time. The “STEM Clustering Method” served as the primary clustering algorithm, with a maximum of 50 models and a maximum variation of 2 between time points.

Suspension liquid chip data analysis

The plasma samples from patients with AP were analyzed on the Luminex100™ I suspension liquid chip platform utilizing data from previous publications⁴. Initially, thirty cytokines linked to the severity of acute pancreatitis were carefully chosen for subsequent analysis.

Common targets

Through the integration of RNA-Seq and liquid microarray data, genes displaying a progressive expression pattern over time were identified using STEM analysis and compared with 30 cytokines linked to the severity of AP.

Data analysis and visualization were conducted using the bioinformatics platform available at <https://www.bioinformatics.com>. The CN online platform was specifically utilized for data analysis and visualization to generate graphical representations.

Statistics

Statistical analysis was conducted using GraphPad Prism 8.0, and the outcomes were depicted as mean \pm standard deviation (SD). Group distinctions were assessed using a t-test for two groups and a one-way ANOVA for more than two groups. Statistical significance was defined as a P-value < 0.05 .

Results

Transcriptomic analysis of AP combined with suspension liquid chip identified PTX3

To investigate the gene expression profiles during the progression of AP, we analyzed the RNA-Seq data under the time gradient CAE induced AP model. Specifically, we presented the number of up-regulated and down-regulated genes at 3 h, 6 h, and 12 h time points (Fig. 1A). Meanwhile, a volcano plot was drawn (Fig. 1B), and a Venn diagram was utilized to illustrate the intersection of differential genes (Fig. 1C). Subsequently, Gene Ontology (GO) and Kyoto Encyclopedia of Genes and Genomes (KEGG) pathway enrichment analyses were conducted on the common genes (Fig. 1D, F), and the KEGG pathways were further classified and annotated^{11–13} (Fig. 1E). Next, through STEM analysis, three clusters of genes with an upward expression trend were screened out. The expression changes of each gene within these clusters at different time points were visualized using a heat map (Fig. 2A), along with the corresponding GO analysis results (Fig. 2B). Finally, the intersection was

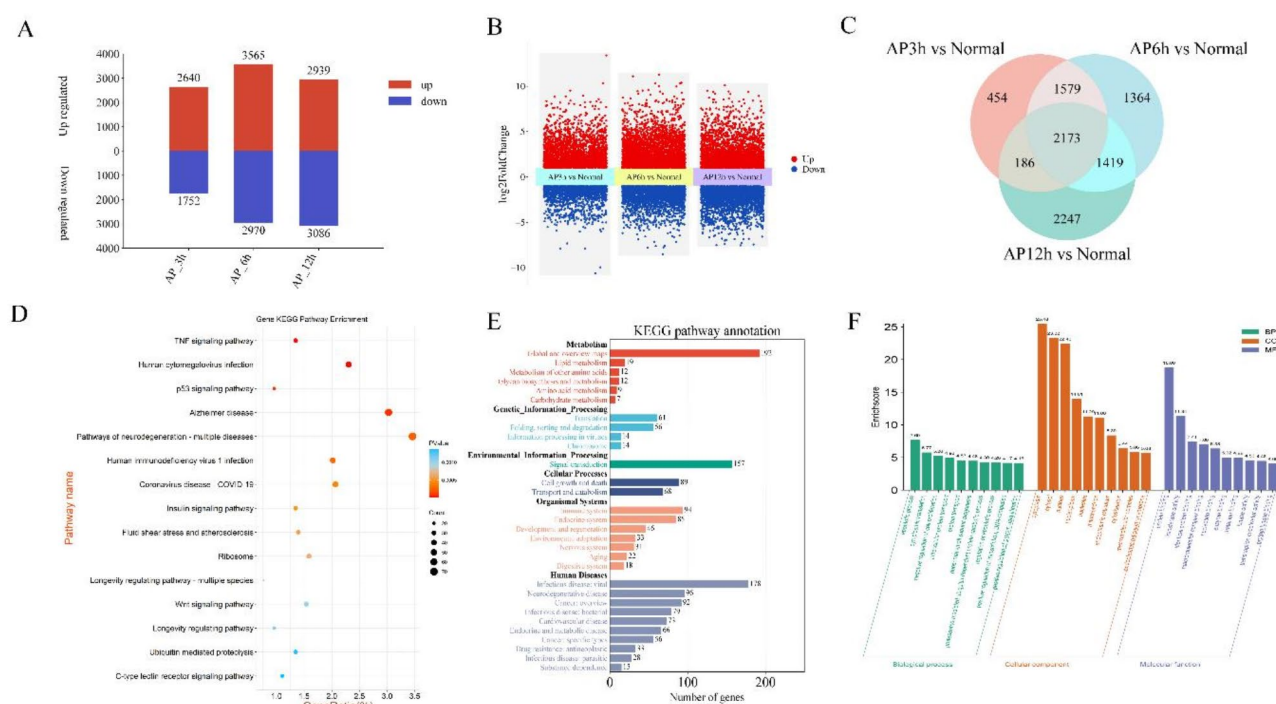


Fig. 1. Transcriptomic analysis of AP. (A) AP transcriptomic gene up-down-regulation histogram. (B) AP transcriptomic volcano map (Screening criteria: FC ≥ 1 P value > 0.05). (C) Wayne diagram of overlapping differential genes at different time periods. (D) KEGG pathway analysis of differential genes. (E) KEGG annotation classification histogram. (F) GO analysis histogram of common differential genes.

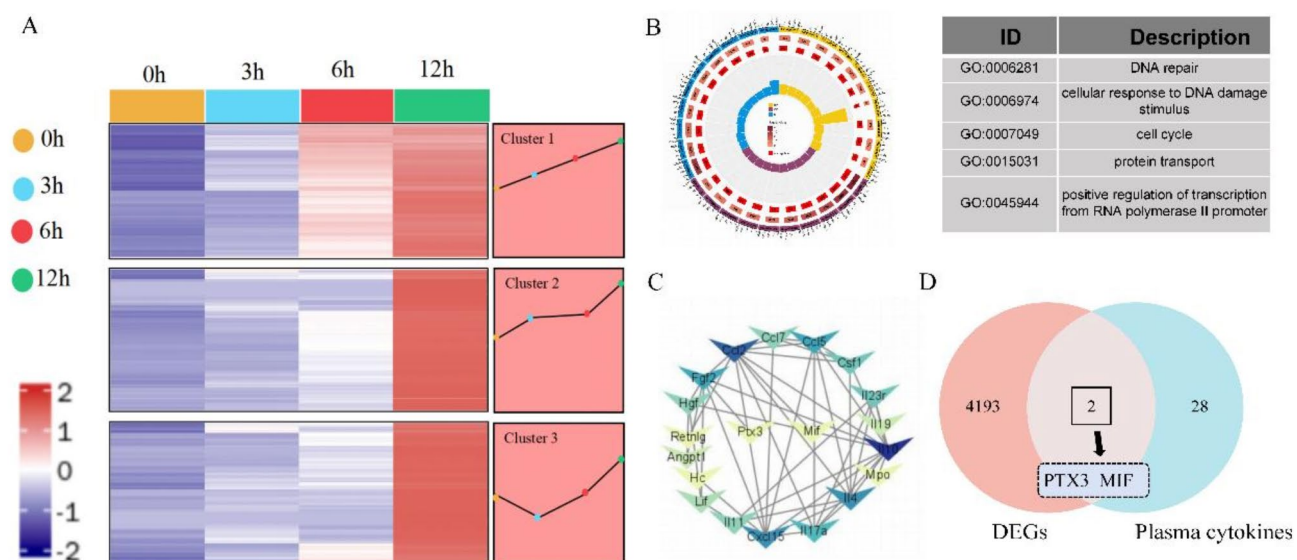


Fig. 2. Transcriptomic analysis of AP combined with suspension liquid chip identified PTX3. **(A)** Heat map and trend map of short time series expression mining (STEM) analysis. **(B)** GO chord plot of gene clusters 1,2,3 and significant enriched GO terms. **(C)** Interaction of AP severity related proteins. **(D)** Common genes of liquid chip and rising trend gene group.

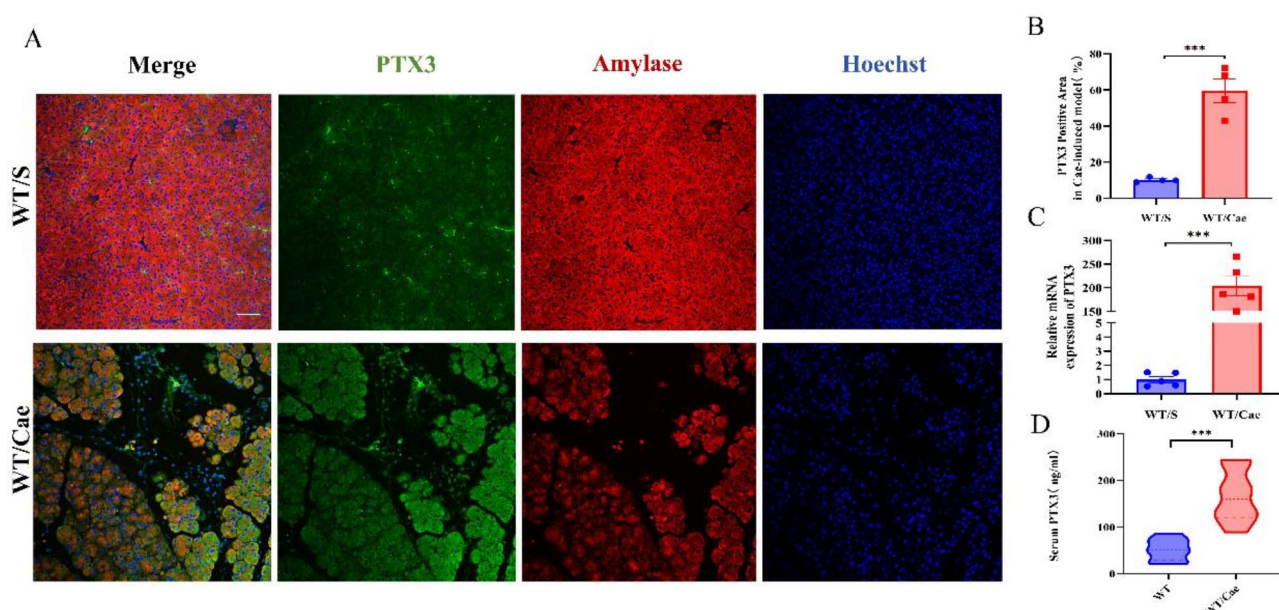


Fig. 3. Expression levels of PTX3 in the AP model. (A) Representative immunofluorescence images of PTX3 expression in pancreatic tissue. (B) Quantitative analysis of immunofluorescence=4, ***p < 0.001. (C) mRNA level of PTX3 in pancreatic tissue. (D) Serum PTX3 level determined by ELISA; **p < 0.01, ***p < 0.001.

taken between 30 plasma cytokines related to the severity of AP disease and 4194 up-regulated genes to display the interaction relationships among plasma factors (Fig. 2C), leading to the identification of PTX3 and MIF (Fig. 2D). Notably, PTX3 exhibited a significant differential expression in transcriptomics.

In conclusion, through the combined analysis of AP transcriptomics and liquid chip technology, it was clearly demonstrated that there is a close association between PTX3 and AP disease.

Expression levels of PTX3 in the AP model

Immunofluorescence and quantitative analysis revealed notable PTX3 overexpression in pancreatic tissue of the AP model (Fig. 3A, B). Additionally, PTX3 mRNA levels exhibited a substantial increase in pancreatic tissue

of AP mice compared to wild-type (WT) mice (Fig. 3C). Furthermore, serum analysis confirmed a significant elevation in PTX3 levels (Fig. 3D). These findings strongly suggested a pronounced upregulation of PTX3 in the AP model induced by CAE.

PTX3 exacerbates pancreatic tissue injury in AP

In order to investigate the impact of PTX3, recombinant PTX3 protein (rPTX3) was intraperitoneally injected to evaluate its effects on AP mice, classified into control, AP, and rPTX3 dose gradient groups (5, 10, 20 ug/kg). The outcomes demonstrated that varying doses of rPTX3 exacerbated pathological injury in AP, evident in tissue edema, heightened neutrophil infiltration, and increased acinar cell necrosis (Fig. 4A-E), with the 10 ug/kg dose exacerbating pancreatic injury to a greater extent. Notably, the rPTX3 groups displayed elevated serum amylase levels, and serum lipase was not statistically significant (Fig. 4F, G). These findings indicated that rPTX3 significantly contributes to the aggravation of pancreatic tissue injury in AP.

PTX3 exacerbates acinar cell damage in AP

Noting that acinar cells constitute over 90% of pancreatic tissue, as cited in literature¹⁴, we explored the direct impact of PTX3 on acinar cells. The vitro experiments revealed that rPTX3 intensified primary acinar cell death

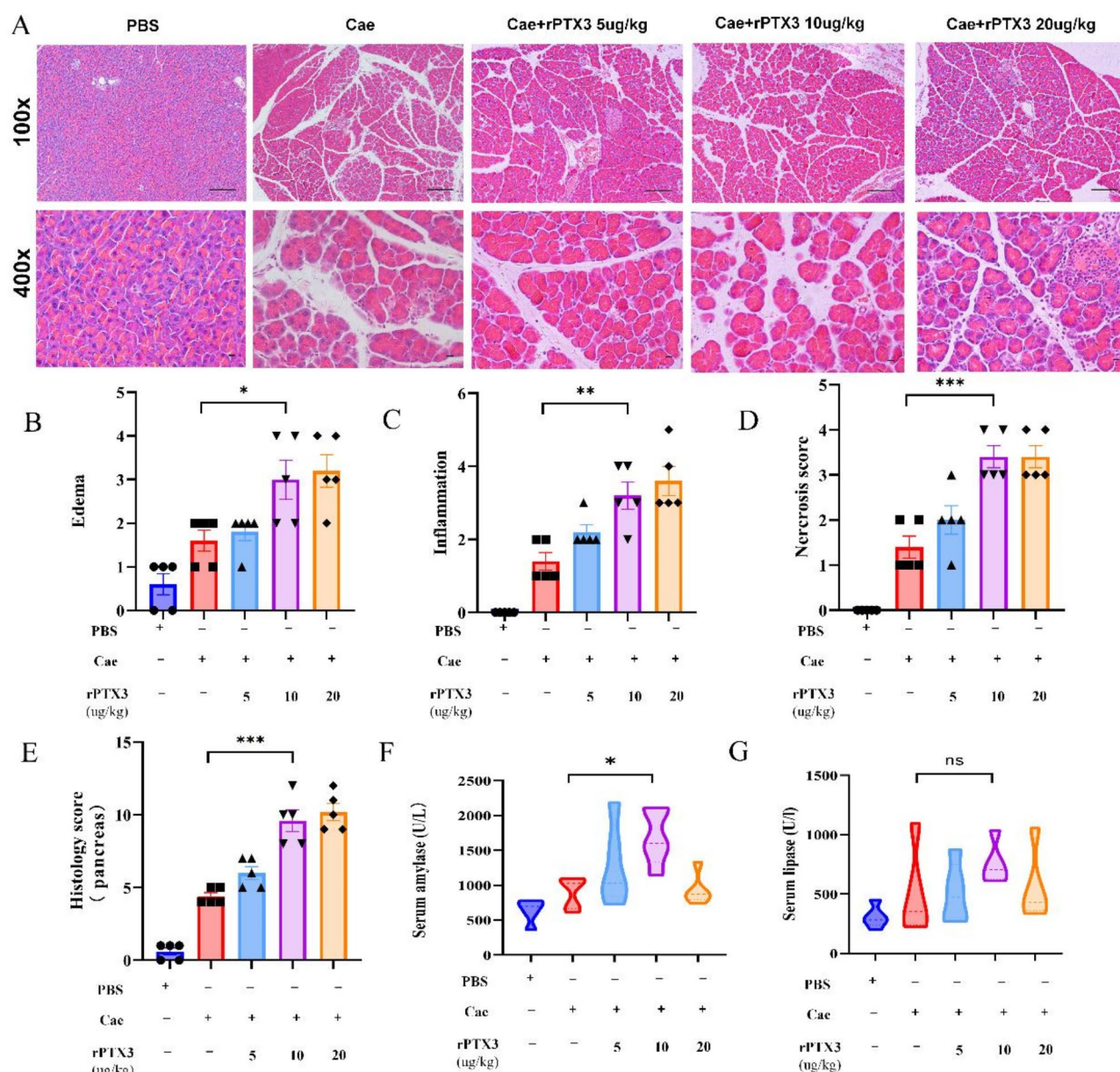


Fig. 4. PTX3 exacerbates pancreatic tissue injury in AP. (A) Representative H&E staining of pancreatic tissue at 100X and 400X magnification. Scale bars, 200/50μm, N=5. (B-E) Histopathological scores of pancreatic tissues, N=5. (F-G) Serum amylase and lipase levels. *p < 0.05, **p < 0.01, ***p < 0.001.

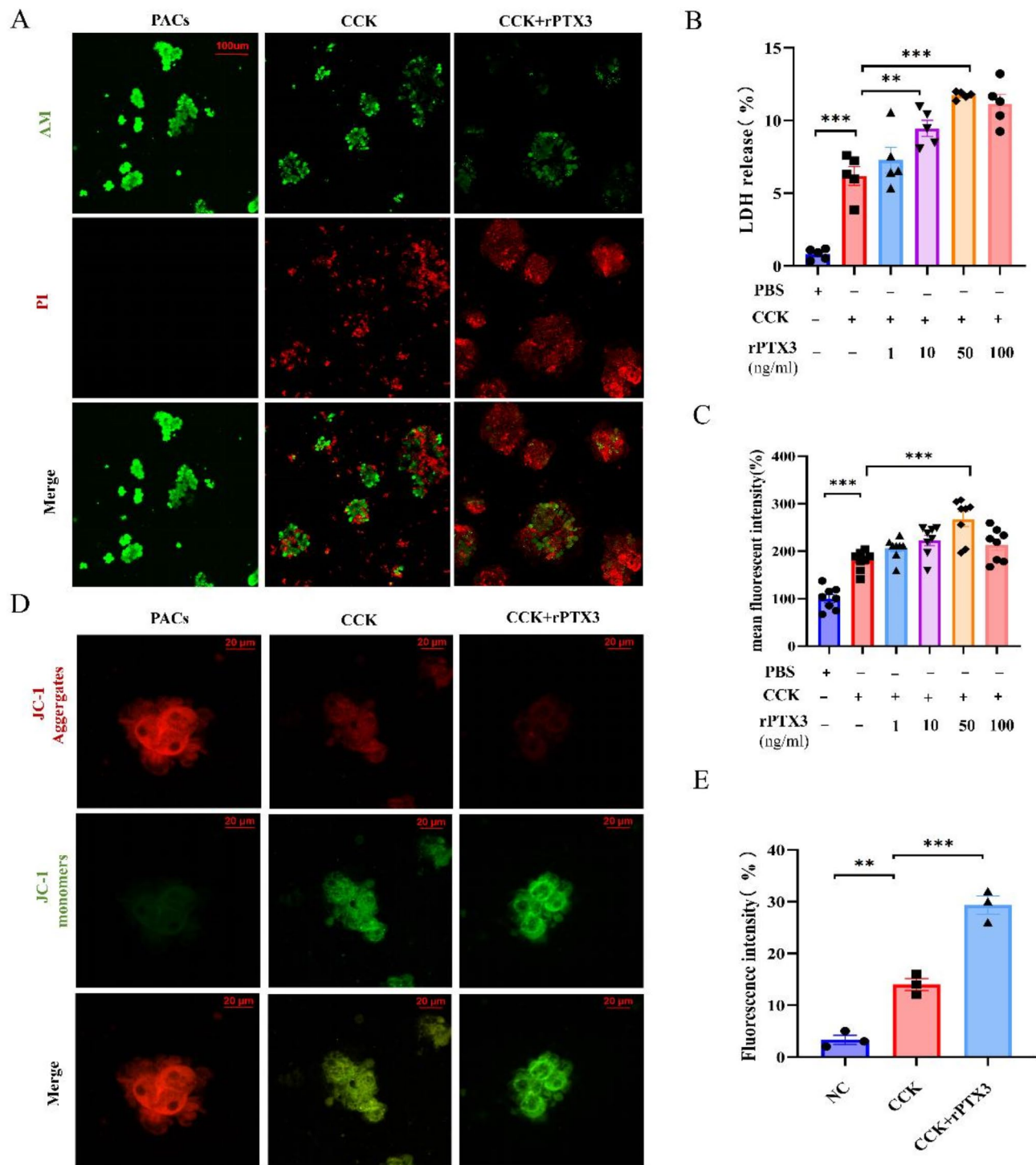


Fig. 5. PTX3 exacerbates acinar cell damage in AP. **(A)** Acinar cell PI/AM live and dead cell double staining, $N=3$. **(B)** Percentage of LDH release in acinous cells (%), $N=5$, $**p<0.01$, $***p<0.001$. **(C)** Average fluorescence intensity produced by ROS in acinous cells, $N=8$, $***p<0.001$. **(D)** Changes in mitochondrial membrane potential of acinous cells after recombinant protein PTX3 intervention. **(E)** Quantitative fluorescence analysis of mitochondrial membrane potential, $N=3$, $*p<0.05$, $**p<0.01$, $***p<0.001$.

detected by acinar cells PI/AM double staining and LDH release (Fig. 5A, B). Previous studies have highlighted the regulation of PTX3 expression by oxidative stress and reactive oxygen species^{15, 16}. Consistent with this, our findings indicated elevated levels of reactive oxygen species in rPTX3 groups, with the most substantial increase observed at 50 ng/ml rPTX3 stimulation (Fig. 5C). Considering the excessive ROS to disrupt mitochondrial membrane potential and exacerbate cellular injury¹⁷, we further analyzed the alteration in mitochondrial

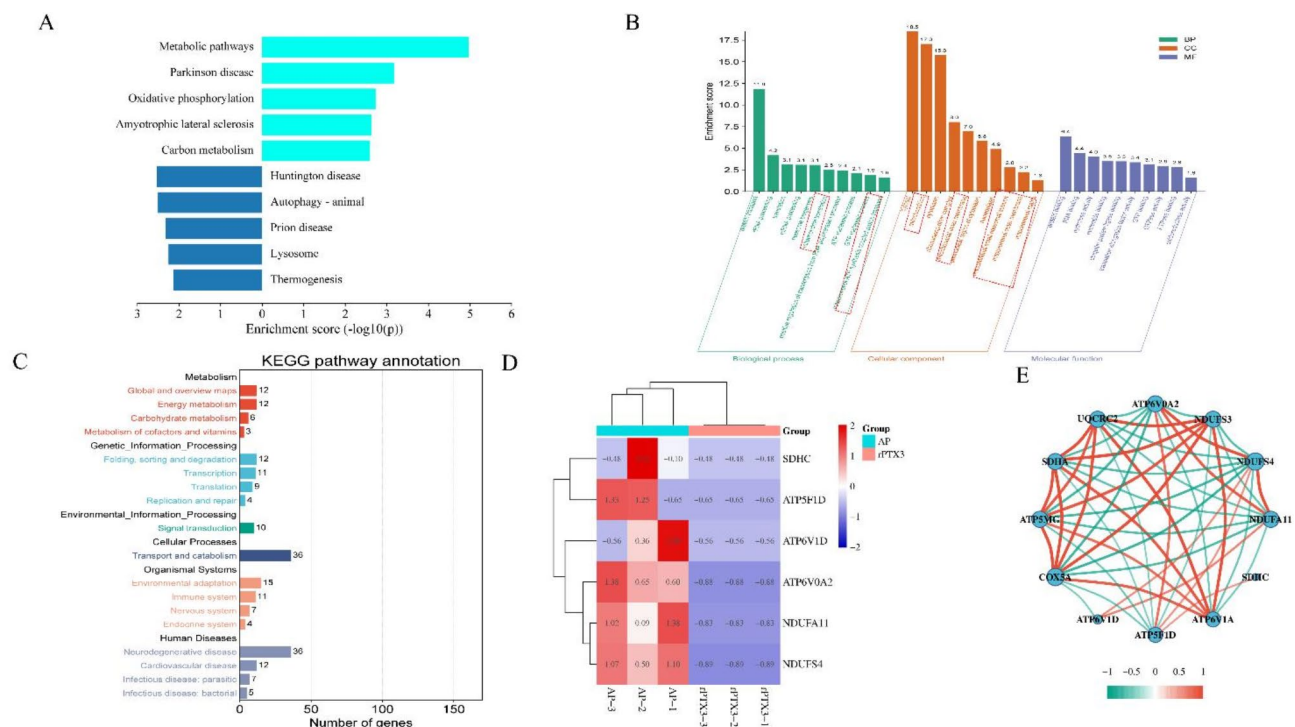


Fig. 6. Proteomics identifies oxidative phosphorylation pathways. (A) KEGG pathway enrichment analysis. (B) GO analysis. (C) KEGG classification annotation. (D) Oxidative phosphorylation pathway differential gene heat map. (E) Oxidative phosphorylation pathway differential gene correlation coefficient analysis.

membrane potential in pancreatic acinar cells. Remarkably, a notable decrease was observed, particularly following the administration of 50 ng/ml recombinant PTX3 (Fig. 5D, E). These findings showed the ability of recombinant PTX3 to worsen acinar cell mortality.

PTX3 mediates the oxidative phosphorylation pathway to exacerbate acinar cell damage

To investigate the mechanism of PTX3 in exacerbating AP damage, KEGG enrichment analysis and classification annotation were conducted (Fig. 6A, C), highlighting the prominent involvement of the oxidative phosphorylation pathway as a notable focus (Fig. 6A). The results of GO analysis on differential genes revealed cellular localization within mitochondria, associated with biological functions of mitochondrial translation and mitochondrial small ribosomal subunit (Fig. 6B). Additionally, the cluster heatmap illustrated genes with the most significant alterations in the oxidative phosphorylation pathway (Fig. 6E), along with correlation coefficient calculations and gene associations (Fig. 6D). Furthermore, the mRNA-level of ATP6V1D, NDUFA11, ATP5F1D, ATP6V0A2, NDUF4, SDHC gene expression verification was performed (Fig. 7A–F). The results showed that except for ATP5F1D and ATP6V0A2, the mRNA expression levels of other genes were decreased, which was consistent with the results of omics.

Furthermore, to further clarify the changes in the oxidative phosphorylation pathway, we stimulated pancreatic acinar cells by Rotenone, one of inhibitors targeting the oxidative phosphorylation pathway. Rotenone effectively blocks the electron transport chain, inhibiting the oxidative phosphorylation process and leading to the obstruction of intracellular ATP synthesis. As shown in Fig. 7G, after blocking the oxidative phosphorylation pathway and intervening with recombinant protein PTX3, we observed that intervention with recombinant protein PTX3 combined with oxidative phosphorylation inhibitor had no significant difference in damage to pancreatic acinar cells compared with intervention with inhibitor alone (Fig. 7G). This finding showed that the oxidative phosphorylation pathway plays a critical role in PTX3-induced acinar cell damage.

Discussion

This study initially focused on the role of PTX3 in acinar cell injury within AP. As previous clinical data indicated a significant elevation in PTX3 levels in the peripheral blood of AP patients, the multi-omics data and experimental validation in our study also highlighted the heightened expression of PTX3 in pancreatic tissue in AP model induced by CAE. Moreover, both the experiments in vitro and in vivo experiments demonstrated that recombinant PTX3 intensifies damage to pancreatic tissue and acinar cells. And, there was potential for the oxidative phosphorylation pathway as the underlying mechanism for PTX3-mediated acinar cell injury in AP.

PTX3 exhibited an increasing trend in the early 24 to 48 h period and proved to be a more effective serum marker for predicting the severity of severe acute pancreatitis (SAP) compared to conventional scores⁴. A combination of nutritional support and insulin therapy significantly reduced the serum PTX3 levels in patients suffering from diabetic ketoacidosis and AP¹⁸. These findings signified the close association of PTX3 with AP, yet the

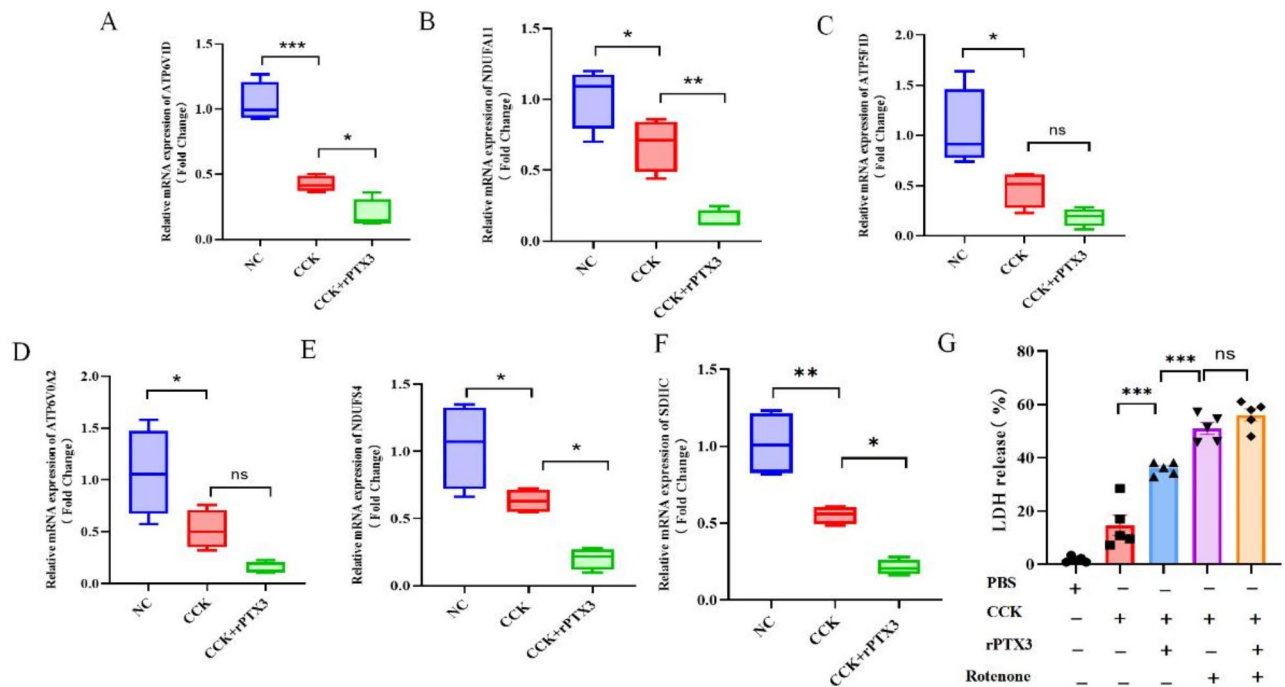


Fig. 7. mRNA levels of validated gene with significant changes in oxidative phosphorylation pathways. (A–F) mRNA levels of differential genes, $N=4$, * $p < 0.05$, ** $p < 0.01$, *** $p < 0.001$. (G) Percentage of LDH release in acinous cells after oxidative phosphorylation inhibitor rotenone intervention, $N=5$, ** $p < 0.01$, *** $p < 0.001$.

underlying biological functionalities and mechanisms warrant further exploration. Our research demonstrated markedly elevated levels of PTX3 in the pancreas and serum. Additionally, vitro and vivo investigations unveiled that intervention with PTX3 recombinant protein could exacerbate pancreatic tissue and acinar cell damage in AP. This aligned with prior research indicating the detrimental effects of PTX3, where PTX3 overexpression aggravated LPS-stimulated proptosis and NLRP3 inflammasome activation in human periodontal ligament stem cells¹⁹. Furthermore, PTX3 was found to escalate the inflammatory response in psoriasis-like dermatitis²⁰.

Intracellular calcium overload and reduced ATP production in mitochondria contribute to pancreatic necrosis in AP²¹. Calcium overload or elevated reactive oxygen species levels can trigger the opening of the mitochondrial permeability transition pore, resulting in diminished mitochondrial membrane potential, cellular swelling, and ultimately rupture²². Our observations demonstrated a reduction in mitochondrial membrane potential and an increase in reactive oxygen species production in acinar cells through fluorescent staining. Meanwhile, the proteomic KEGG analysis in this study suggested that PTX3 may play a role in modulating the oxidative phosphorylation pathway in AP, thereby exacerbating pancreatic injury.

Oxidative phosphorylation is the process where energy from oxidation drives the phosphorylation of ADP to generate ATP²³. PTX3 may disrupt this process by inhibiting the electron transport chain. It can cause electron leakage, leading to the production of ROS, such as superoxide anions. These ROS can further convert into other reactive species, increasing intracellular ROS levels²⁴. Additionally, PTX3-induced electron transfer blockage disrupts the mitochondrial membrane potential, impairing mitochondrial function and ATP synthesis efficiency, ultimately triggering mitochondrial dysfunction²⁵.

However, there were several limitations should be noted. Firstly, this study did not further investigate the effect of endogenous PTX3 deficiency on AP pancreatic injury in mice. The lack of validation using PTX3-KO mice may somewhat limit the broader applicability of our study. Additionally, we did not explore the challenges related to therapeutic translation targeting PTX3 such as studies on PTX3 inhibitors or small interfering RNA intervention. Finally, a comprehensive investigation of PTX3's involvement in mediating the oxidative phosphorylation pathway in AP was needed.

Currently, there is no product of PTX3 inhibitors. In the transition from basic research to clinical application, the future development of PTX3 inhibitors may serve as a potential therapeutic target for intervening in pancreatic necrosis associated with AP. By modulating the levels of PTX3 or the activity of its receptors, it may help alleviate inflammatory responses and inhibit excessive immune reactions, thereby providing new strategies for the treatment of related diseases. PTX3 is considered a potential biomarker for early diagnosis and monitoring disease progression. By tracking changes in PTX3 levels, it can help assess disease activity and severity.

In conclusion, this research demonstrated that PTX3 may exacerbate acinar cell damage in AP by modulating the oxidative phosphorylation pathway. In the future, the research and development of PTX3 inhibitors may be expected to provide a new direction for clinical treatment.

Data availability

The original RNA-Seq transcriptome data has been deposited to National Center for Biotechnology Information (NCBI) under the BioProject number PRJNA 1219994. The mass spectrometry proteomics data have been deposited to the ProteomeXchange Consortium (<https://proteomecentral.proteomexchange.org>) via the iProX partner repository with the dataset identifier PXD060566.

Received: 29 September 2024; Accepted: 17 February 2025

Published online: 26 February 2025

References

1. Mederos, M. A., Reber, H. A. & Girgis, M. D. Acute Pancreatitis: A Review. *Jama* **325**, 382–390 (2021).
2. Rashid, M. U. *et al.* Pancreatic necrosis: Complications and changing trend of treatment. *World J. Gastrointest. Surg.* **11**, 198–217 (2019).
3. Jiang, X. *et al.* Drug discovery and formulation development for acute pancreatitis. *Drug Deliv.* **27**, 1562–1580 (2020).
4. Deng, L. H. *et al.* Plasma cytokines can help to identify the development of severe acute pancreatitis on admission. *Medicine* **96**, e7312 (2017).
5. Daigo, K., Mantovani, A. & Bottazzi, B. The yin-yang of long pentraxin PTX3 in inflammation and immunity. *Immunol. Lett.* **161**, 38–43 (2014).
6. Chen, J., Matzuk, M. M., Zhou, X. J. & Lu, C. Y. Endothelial pentraxin 3 contributes to murine ischemic acute kidney injury. *Kidney Int.* **82**, 1195–1207 (2012).
7. Real, J. M. *et al.* Pentraxin 3 accelerates lung injury in high tidal volume ventilation in mice. *Mol. Immunol.* **51**, 82–90 (2012).
8. Hwang, N., Kwon, M.-Y., Cha, J. B., Chung, S. W. & Woo, J. M. Tunicamycin-induced endoplasmic reticulum stress upregulates the expression of pentraxin 3 in human retinal pigment epithelial cells. *Korean J. Ophthalmol. KJO* **30**, 468–478 (2016).
9. Schmidt, J. *et al.* A better model of acute pancreatitis for evaluating therapy. *Ann. Surg.* **215**, 44–56 (1992).
10. Gukovskaya, A. S. *et al.* Pancreatic acinar cells produce, release, and respond to tumor necrosis factor- α . Role in regulating cell death and pancreatitis. *J. Clin. Invest.* **100**, 1853–1862 (1997).
11. Kanehisa, M. Toward understanding the origin and evolution of cellular organisms. *Protein Sci.* **28**, 1947–1951 (2019).
12. Kanehisa, M. & Goto, S. KEGG: Kyoto encyclopedia of genes and genomes. *Nucleic Acids Res.* **28**, 27–30 (2000).
13. Kanehisa, M., Furumichi, M., Sato, Y., Kawashima, M. & Ishiguro-Watanabe, M. KEGG for taxonomy-based analysis of pathways and genomes. *Nucleic Acids Res.* **51**, D587–D592 (2023).
14. Pin, C. L., Ryan, J. F. & Mehmood, R. Acinar cell reprogramming: A clinically important target in pancreatic disease. *Epigenomics* **7**, 267–281 (2015).
15. Garlanda, C., Bottazzi, B., Magrini, E., Inforzato, A. & Mantovani, A. PTX3, a Humoral pattern recognition molecule, in innate immunity, tissue repair, and cancer. *Physiol. Rev.* **98**, 623–639 (2018).
16. Hwang, N., Kwon, M. Y., Woo, J. M. & Chung, S. W. Oxidative stress-induced pentraxin 3 expression human retinal pigment epithelial cells is involved in the pathogenesis of age-related macular degeneration. *Int. J. Mol. Sci.* **20**, (2019).
17. Zorov, D. B., Juhaszova, M. & Sollott, S. J. Mitochondrial reactive oxygen species (ROS) and ROS-induced ROS release. *Physiol. Rev.* **94**, 909–950 (2014).
18. Yin, C. *et al.* Effects of nutritional support combined with insulin therapy on serum proteins, inflammatory factors, pentraxin-3, and serum amylase levels in patients with diabetic ketoacidosis complicated with acute pancreatitis. *Medicine* **100**, e27920 (2021).
19. Han, B. *et al.* Long pentraxin PTX3 deficiency worsens LPS-induced acute lung injury. *Intensive Care Med.* **37**, 334–342 (2011).
20. Liu, J. *et al.* Pentraxin 3 exacerbates psoriasiform dermatitis through regulation of macrophage polarization. *Int. Immunopharmacol.* **130**, 111805 (2024).
21. Petersen, O. H., Gerasimenko, J. V., Gerasimenko, O. V., Gryshchenko, O. & Peng, S. The roles of calcium and ATP in the physiology and pathology of the exocrine pancreas. *Physiol. Rev.* **101**, 1691–1744 (2021).
22. Maléth, J. & Hegyi, P. Ca²⁺ + toxicity and mitochondrial damage in acute pancreatitis: translational overview. *Philos. Trans. R. Soc. Lond. Ser. B, Biol. Sci.* **371**, (2016).
23. Lowy, R. Oxidative phosphorylation. *Biol. Med.* **48**, 110–158 (1959).
24. Nolfi-Donagan, D., Braganza, A. & Shiva, S. Mitochondrial electron transport chain: Oxidative phosphorylation, oxidant production, and methods of measurement. *Redox Biol.* **37**, (2020).
25. Raimundo, N. Mitochondrial pathology: stress signals from the energy factory. *Trends Mol. Med.* **20**, 282–292 (2014).

Author contributions

Wenyue Wang: conceptualization, methodology, investigation, data curation, visualization, writing-original draft. Yaning Wang: investigation, data curation, visualization, writing-original draft. Chenchen Yuan: conceptualization, methodology, investigation, data curation, visualization supervision, project administration. Fei Cao: methodology, investigation. Weisong Tang: methodology, validation. Qingtian Zhu: methodology, validation. Xiaowu Dong: supervision, project administration. Lihui Deng: investigation. Guotao Lu: conceptualization, resources. Qing Xia: supervision. Weiwei Chen: conceptualization, writing – review & editing, supervision, project administration, funding acquisition.

Funding

This study was supported by the National Natural Science Foundation (No.82004291); 333 High-Level Talents Training Project of Jiangsu Province and Six Talent Peaks Project of Jiangsu Province (No.WSN-11325).

Declarations

Ethics approval and consent to participate

All animal experiments were conducted in accordance with the Principles of Laboratory Animal Care (NIH publication 85Y23, revised 1996), and were approved by Science and Technology Commission of the Medical College of Yangzhou University (YXYLL-2024-074).

Competing interests

The authors declare no competing interests.

Disclosure

The authors report there are no competing interests to declare.

Additional information

Correspondence and requests for materials should be addressed to W.C.

Reprints and permissions information is available at www.nature.com/reprints.

Publisher's note Springer Nature remains neutral with regard to jurisdictional claims in published maps and institutional affiliations.

Open Access This article is licensed under a Creative Commons Attribution-NonCommercial-NoDerivatives 4.0 International License, which permits any non-commercial use, sharing, distribution and reproduction in any medium or format, as long as you give appropriate credit to the original author(s) and the source, provide a link to the Creative Commons licence, and indicate if you modified the licensed material. You do not have permission under this licence to share adapted material derived from this article or parts of it. The images or other third party material in this article are included in the article's Creative Commons licence, unless indicated otherwise in a credit line to the material. If material is not included in the article's Creative Commons licence and your intended use is not permitted by statutory regulation or exceeds the permitted use, you will need to obtain permission directly from the copyright holder. To view a copy of this licence, visit <http://creativecommons.org/licenses/by-nc-nd/4.0/>.

© The Author(s) 2025